

# **Metal-Hydrogen Phase Diagrams in the Vicinity of Melting Temperatures**

**V.I. Shapovalov**

Sandia National Laboratories, P.O. Box 5800 Albuquerque, New Mexico 87185-1134

## **Abstract**

Hydrogen-metal interaction phenomena belong to the most exciting challenges of today's physical metallurgy and physics of solids due to the uncommon behavior of hydrogen in condensed media and to the need for understanding hydrogen's strong negative impact on properties of some high-strength steels and alloys. The paper cites and summarizes research data on fundamental thermodynamic characteristics of hydrogen in some metals that absorb it endothermally at elevated temperatures. For a number of metal-hydrogen systems, information on some phase diagrams previously not available to the English-speaking scientific community is presented.

## **Introduction**

A phase diagram not only represents fundamental thermodynamic characteristics of the interacting elements and phases but also provides basic information needed to engineer processes of melting, solidification and heat treatment and to determine alloy service conditions. Research in this important area has been hindered by the well-known difficulties involved in experimentation with hydrogen at elevated temperatures. With the limited amount of information available on high-temperature interactions of hydrogen with some metals of great practical importance, a task was set to determine phase diagrams for the systems Fe-H, Ni-H, Co-H, Cr-H, Mn-H, Cu-H, Al-H, Mg-H, Be-H, Mo-H and W-H. The diagrams used original or refined data on hydrogen solubility together with new findings on the effects of hydrogen on metal melting temperature and transformation temperatures.

## **Experimental**

A number of techniques were developed by the present writer that enable investigations into metal-hydrogen systems over broad ranges of temperature and pressure. Experimental apparatuses were made in several configurations/modifications. The basic units enable heating, cooling, holding and quenching in a vacuum or in an atmosphere of hydrogen, helium, argon, nitrogen or their mixtures, together with thermal analysis and DTA at temperatures up to 2300 K and pressures as high as 100 MPa.

The materials used were at least 99.95 % pure. Hydrogen — or helium or argon in control or special runs — was pressurized above 20 MPa with a membrane pump specially designed to prevent gas contamination during pressurizing. The control runs were performed in ultra pure hydrogen prepared by filtration of commercial hydrogen through palladium membranes.

Furthermore, specialized apparatuses were developed and made that enabled preset holding, quenching, thermal analysis or magnetic tests. A refined technique for hydrogen determination was developed that improved the accuracy of hydrogen solubility measurements by an order of magnitude.

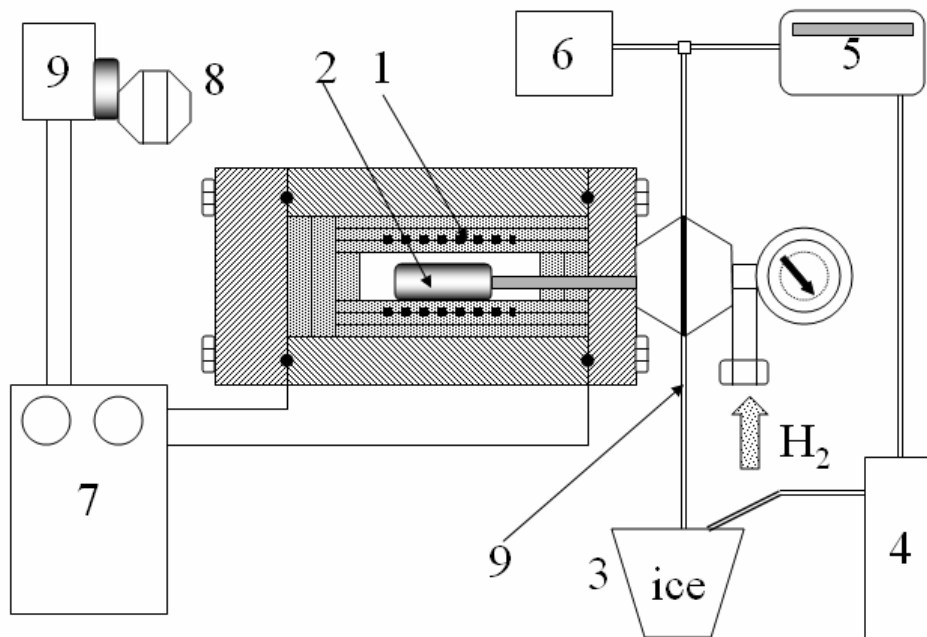
Instruments from LECO, Balzers, Niaphot and Cameca were used in the experiments. Also employed were conventional methods of quantitative metallurgy, hydrostatic weighing, selective etching by thermal, chemical and electrochemical techniques, micro hardness measurements and tensile tests.

The experimental procedures were modified depending on the chemical nature of the metal at hand. For this reason, sections dedicated to individual systems may contain information on features of the experimental techniques.

## The Iron-Hydrogen System

Previous research on the Fe-H system was mostly focused on hydrogen solubility in iron. On the other hand, data on how hydrogen influences the melting temperature and the allotropy are very scarce. W. Geller and Tak-Hosun tried to assess the Fe-H diagram for a hydrogen pressure of 0.1 MPa, using the existing data on hydrogen solubility and the general thermodynamic relationships [1]. It was concluded that hydrogen reduces the melting temperature by 1.8 K and extends the  $\gamma$  region. It was observed even earlier that the  $\alpha$ - $\gamma$  equilibrium temperature drops by 4 K in the presence of hydrogen [2].

The present writer investigated the effects of hydrogen on iron transformation temperatures at pressures up to 90 MPa and temperatures ranging from 500 to 1600 °C [3].



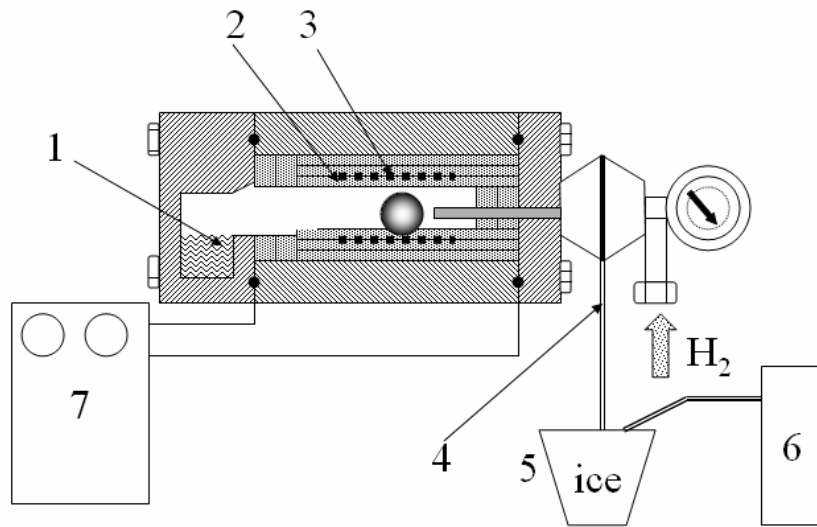


**Figure 1.** Apparatus for studies into the effects of hydrogen on metal transformation temperatures. 1: heating element, 2: specimen, 3: ice water vessel, 4: galvanometer, 5: potentiometer, 6: balance galvanometer, 7, 9: voltage regulators, 8: synchronous motor with gear box.

**Figure 2.** Apparatus for charging metals with hydrogen and quenching in water. 1: water, 2: heating element, 3: specimen, 4: thermocouple, 5: ice water vessel, 6: potentiometer, 7: voltage regulator.

Figure 1 shows the experimental apparatus used in the study. The high pressure chamber made of austenitic stainless steel had a water-cooled casing and covers. Resistance furnaces with molybdenum or tungsten heating elements were used. The chamber walls had a thermal insulation of quartz washers and alumina tubes. Thermal analysis and DTA was used to determine the transformation temperatures in heating. W-Re thermocouples in alumina sheaths served as sensors. The electromotive force of a plain thermocouple was measured with a Class 0.05 galvanometer enabling a precision of 1 K; for a differential thermocouple, a balance galvanometer was used. The gas pressure was measured with a pressure gage to an accuracy not less than 2 %. The hydrogen gas of commercial purity was supplied in cylinders. The gas composition was checked with a chromatograph.

High-pure iron with a maximum total amount of impurities at 0.002 % was prepared for the experiments by induction melting of carbonyl iron in an alumina crucible and an atmosphere of hydrogen. The liquid iron was then held 1 h in argon for degassing. An ingot about 350 g in weight was cut and forged to rods 15 mm in diameter which were next machined to cylinders 12 mm in diameter and 16 mm long. These were cut lengthwise, and a hole 2 mm in diameter and 10 mm deep was drilled in each of the halves to allow insertion of a thermocouple. Molybdenum specimens were used for reference. An iron sample was degassed together with a reference specimen in a vacuum at 800 °C for 5 h. Next, the two specimens together with a thin quartz plate interposed for thermal insulation were placed into the experimental chamber. In order to attain the closest possible proximity to the gas-metal equilibrium, the iron specimens for some runs were stacked up from plates 0.5 mm thick made by rolling at room temperature.

The saturation time at 900 °C was 300 s for a solid specimen and not longer than 10 s for a stacked specimen. At higher temperatures, the saturation time lengths were even shorter. With this in mind, the rates of heating and cooling were varied in the range from 1 to 100 K/min.

The experimental data were practically the same for the two specimen types because preliminary saturation with hydrogen was carried out in the vicinity of phase transformation temperatures. The heating and cooling curves were obtained simultaneously with differential curves. Several replications

were run for each experimental point (10 to 15). No cooling curves were used to determine phase diagrams because of marked super cooling in phase transformations.

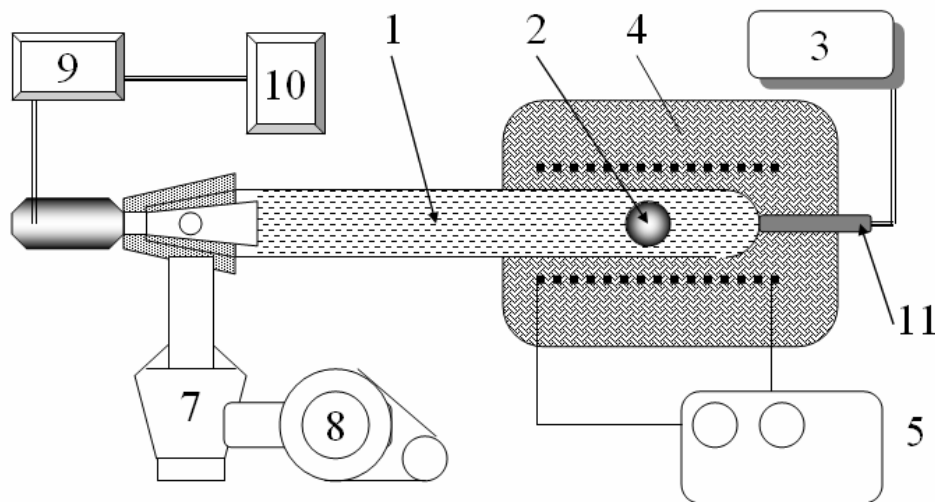


Figure 3. Apparatus for hydrogen determination by cyclic vacuum extraction. 1: reaction tube, 2: specimen, 3: galvanometer, 4: furnace, 5: voltage regulator, 6: pressure sensor, 7: diffusion pump, 8: roughing pump, 9: vacuum gage, 10: recorder.

Hydrogen solubility was determined via quenching — so far the only technique available for high temperatures and hydrogen pressures. Fig. 2 gives a schematic of a unit for holding in hydrogen gas and subsequent quenching. The holding temperature was maintained to a precision of 2 K. The saturation time was selected for each temperature by trial and error. When the equilibrium was attained, the furnace was rotated, so that the specimen was abruptly dropped into the quenching section filled with ice water. When the experimental temperature was above the melting point, the molten iron flowed into the quenching section via a quartz tube. The average cooling rate in water was about 300 K/s.

The hydrogen content was measured by vacuum extraction directly after quenching. In order to improve the accuracy of measurements, a special apparatus was designed, Fig. 3. It eliminated the main disadvantage of Sieverts method, namely equilibration between the solute and the gaseous hydrogen during the vacuum extraction. This disadvantage was corrected via cyclic degassing. On reaching an internal pressure of 10 Pa, the reaction tube was connected to the vacuum system preevacuated to 0.001 Pa. The hydrogen that had released was removed in a few seconds, the reaction chamber was again isolated from the vacuum system, and the release of hydrogen was resumed under a high vacuum. The absolute accuracy of hydrogen measurement for a 450 cm<sup>3</sup> reaction tube was 0.03 cm<sup>3</sup>. The corrections for possible hydrogen release during specimen quenching were negligible at less than 1 %. The interval between the quenching and the degassing step was not longer than 5 min. An estimated 0.5 % hydrogen could release from a spherical specimen 15 g in weight at room temperature. The bake-out was carried out stepwise: first at 300 °C, next at 800 °C. At least 80 % of the hydrogen evolved at 300 °C. The correction for residual hydrogen due to vacuum melting was 0.05 cm<sup>3</sup>. To estimate the side effects of quenching, namely possible iron charging with hydrogen, oxygen and nitrogen during contact of hot specimen with water, the unit was filled with helium at a similar pressure. The amount of these gases was found to range from 0.1 to 0.3 cm<sup>3</sup> per 100 g iron.

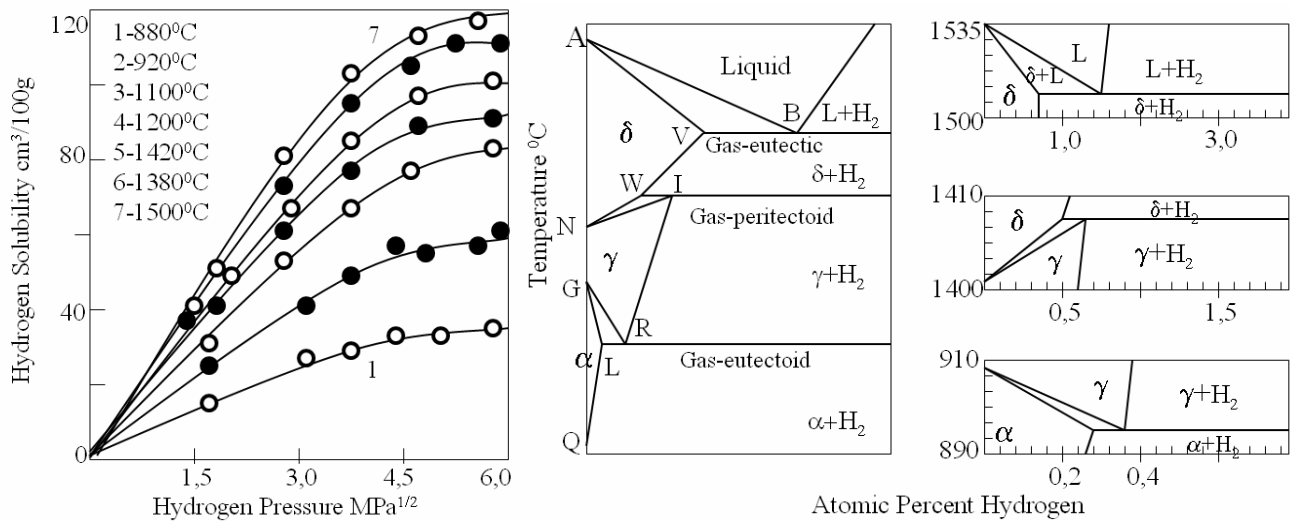


Figure 4. Effects of temperature and pressure on hydrogen solubility in iron.

Figure 5. Proposed Fe-H phase diagram for 40 MPa pressure. General view of the Fe-rich portion (left) and the major nodes (right).

It was found that hydrogen reduces iron melting temperature and expands the temperature range of gamma iron stability, see Fig. 5. These findings are in qualitative agreement with earlier estimates; moreover, quantitative agreement was observed for the melting temperature drop at 0.1 MPa [1]. However, the transformation temperature shifts show little agreement with the earlier theories, the estimated values being 4 to 5 times greater than the experimental ones. Our findings therefore reveal that at low pressures hydrogen does not much affect the transformation temperatures of iron. Its influence becomes appreciable from 2 or 3 MPa.

Remarkably, the curve slopes are changed at pressures of 20 to 25 MPa, so that increasing the pressure is accompanied by only negligible shifts in the transformation temperatures. Based on a comparison of these results with the data on the effects of pressure on hydrogen solubility, see Fig. 4, the above phenomena may be associated with deviations from the Sieverts' square root law at pressures exceeding 10 MPa [4].

From a comparison of our data on hydrogen solubility and hydrogen effects on the values of transformation temperatures of iron, it may be concluded that what is called a "limiting" Fe-H phase diagram should exist because there are natural limitations on hydrogen solubility in iron and therefore the shifts of transformation temperatures are limited. Fig. 5 shows a version of such a diagram. The diagram shows that hydrogen effects on the transformation temperatures are similar in nature to those of carbon and nitrogen. In terms of their averaged molar fractions, hydrogen, carbon and nitrogen display similar impacts on behavior of liquid solutions and austenite, although hydrogen influences alpha and delta ferrite much less. The above diagram shows three invariant equilibria, namely VB the gas-eutectic, WJ the gas-peritectoid and LR the gas-eutectoid one.

The severe deviations from Sieverts law may be caused by saturation of the iron lattice with hydrogen, for it is clear that no complete solubility is possible in the Fe-H system. It must resemble the systems Fe-C and Fe-N in this respect. The negative deviations are balanced out by a superior absorbing capacity of lattice defects like grain boundaries, dislocation piles and microdefects. It is possible that above some pressure the hydrogen content would be greater at lower temperatures than at higher ones. This peculiar combination of the effects of pressure and temperature on the solubility would result in an inflected line of hydrogen partial solubility in ferrite (LQ). It should be noted, however, that this statement on an equilibrium nature of the LQ line is open to discussion.

It is worthwhile dwelling on the data on hydrogen solubility in delta iron. The characteristics of solubility in this allotropic form turned out to be much different from those in alpha iron. For example, the heat of solution of hydrogen in delta iron was found to be 2.5 times that in alpha iron. Earlier, it was believed that the solution behavior in the two polymorphs should be similar because of their similar crystal structure. The above data testify to inherent differences in the physical chemistry of alpha and delta iron. After all, the occurrence of similar lattices in so distant temperature regions in itself should indicate their difference.

### The Systems Nickel-Hydrogen and Cobalt-Hydrogen

Although studies into hydrogen interactions with nickel- and cobalt-base materials are topical, such data are still lacking in the available literature [5]. This may be a reason why no information on the respective phase diagrams could be found for quite a long time.

The experimentation was performed using units described above, see Figs. 1- 3 . Hydrogen solubility measurements were carried out in the ranges from 500 to 1500 °C and 0.1 to 50 MPa by the method described for iron. The influence of hydrogen on melting temperatures of nickel and cobalt was investigated by the thermocouple circuit break technique. Its advantage over the thermal analysis lies in the possibility of using specimens shaped as very thin wires in which the gas-metal equilibrium is attained fairly rapidly. In the experiments at hand, a wire 0.1 mm thick and 3 to 4 mm long was connected in series with a W-Re thermocouple and placed into the zone of gradient-free heating. While heating the specimen at 2 K/min, potentiometer readings were followed. The circuit was broken at the instant of melting, and the corresponding reading was taken to be the melting temperature. Thermal analysis as employed for the Fe-H system was also used to check this technique, and the results were practically identical. At least 20 measurements of melting temperature were taken, the reproducibility and scatter allowing an accuracy of 2 K.

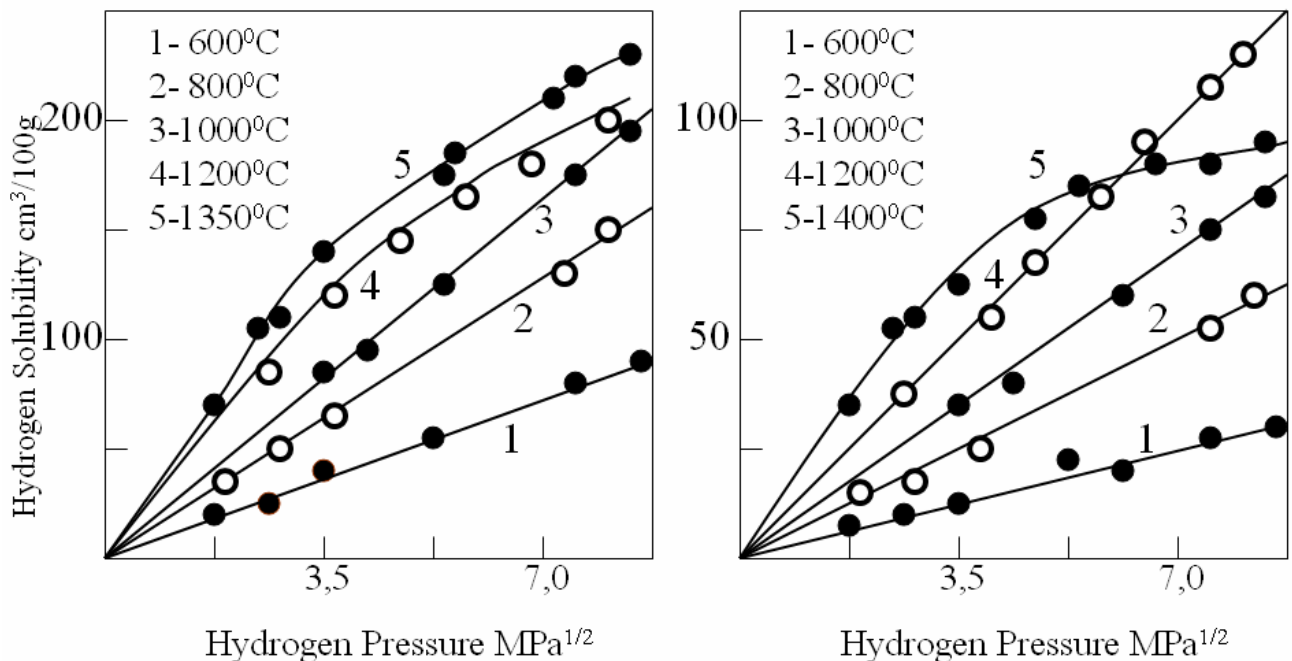


Figure 6. Effects of temperature and pressure on hydrogen solubility in nickel and cobalt. 1: 600 °C, 2: 800 °C, 3: 1000 °C, 4: 1200 °C, 5 (Ni): 1350 °C, 5 (Co): 1400 °C.

The experiments revealed that the solubility of hydrogen in nickel or cobalt is increased with increasing temperature and pressure (Fig. 6), while their melting temperatures decline with rising hydrogen pressure, Fig. 7. At temperatures in excess of 1200 °C, both metals exhibit negative deviations from the Sieverts law similar to those described above for iron. Therefore, “limiting” phase diagrams may exist for the Ni-H and Co-H systems, as is the case with the Fe-H system. High-temperature portions of the two diagrams including the gas-eutectic equilibrium were determined based on the data obtained for hydrogen solubility and hydrogen effects on the melting temperatures, Fig. 8.

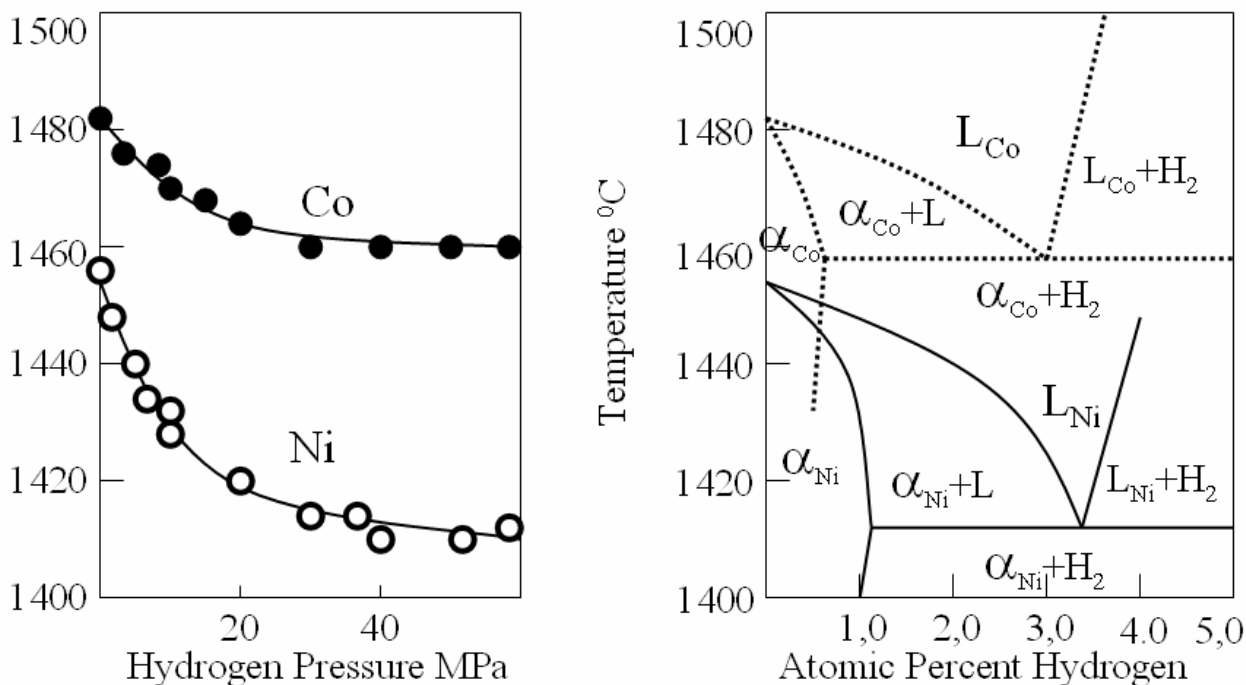


Figure 7. Influence of hydrogen pressure on melting temperature of cobalt (1) and nickel (2).

Figure 8. Phase diagrams of the Co-H (top) and the Ni-H system (bottom) for pressures below 50 MPa.

### The Chromium-Hydrogen System

The interactions of hydrogen with chromium are poorly known. Only a few papers are available on hydrogen solubility in this industrially important metal [6, 7].

An investigation into hydrogen solubility in chromium and into the influence of hydrogen on chromium melting temperature was carried out in the range of temperatures from 300 to 1500 °C and pressures up to 10 MPa.

Electrolytic chromium of 99.98 % purity was remelted in a vacuum induction furnace and poured to ingots 250 to 350 g in weight. These were machined to spherical specimens for solubility measurements or to cylindrical ones for thermal analysis runs.

The experimental units and techniques were the same as for the iron-hydrogen system.

Chromium was found to occlude hydrogen exothermally up to 550 °C and endothermally above this temperature, Fig. 10. It therefore cannot be categorized with any of the well-known groups of exothermally occluding, endothermally occluding, hydride-forming or non-hydride-forming elements. This supports a view that some metals should be classified under a special group regarding their interactions with hydrogen [8].

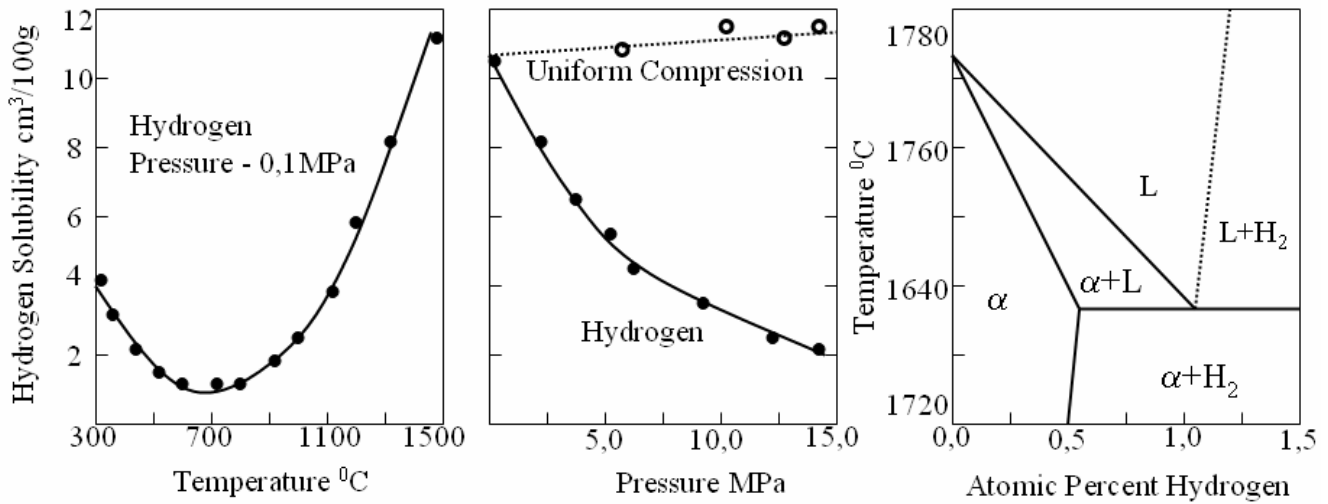


Figure 9. Hydrogen solubility in chromium for 0.1 MPa pressure.

Figure 10. Chromium melting temperature as a function uniform compression (1) and hydrogen pressure (2).

Figure 11. Cr-H phase diagram for hydrogen pressure up to 10 MPa.

Above 600 °C, the solubility of hydrogen in chromium follows Sieverts law over the entire pressure range up to 10 MPa. Different investigators have reported the melting temperature of chromium quite differently within a wide range from 1513 to 1900 °C, which may be explained by different levels of impurities in the samples under study. Our measurements gave the melting temperature value of 1773 °C. As the hydrogen pressure and consequently its content in the metal is increased, the melting temperature drops markedly, Fig. 11. It became possible to determine a partial Cr-H diagram depicted in Fig. 12 using the above experimental data together with some assumptions regarding hydrogen solubility in liquid chromium [6, 7]. With this in mind the liquidus is shown in broken lines. The diagram indicates that a gas-eutectic reaction should occur in the Cr-H system, as is the case in the systems described above.

## The Copper-Hydrogen System

Only a few investigators addressed the Cu-H system. Moreover, an analysis of the literature data revealed that their measurements of hydrogen solubility were in conflict. For example, the reported values of heat of solution varied from 70 to 205 kJ/mol. The absolute values of solubility limit also differed almost by an order of magnitude.

The present studies involved the experimental equipment and techniques described in the section on the Fe-H system. Hydrogen gas pressures from 0.1 to 100 MPa and temperatures from 600 to 1100 °C were used.

It was found that hydrogen solubility in copper is increased with increasing the temperature and/or pressure, Fig. 12. Contrary to iron, nickel and cobalt, copper obeys the Sieverts law over the entire ranges of temperature and pressure. This can be explained by differences in the chemical nature between copper and the above metals belonging to the iron group.

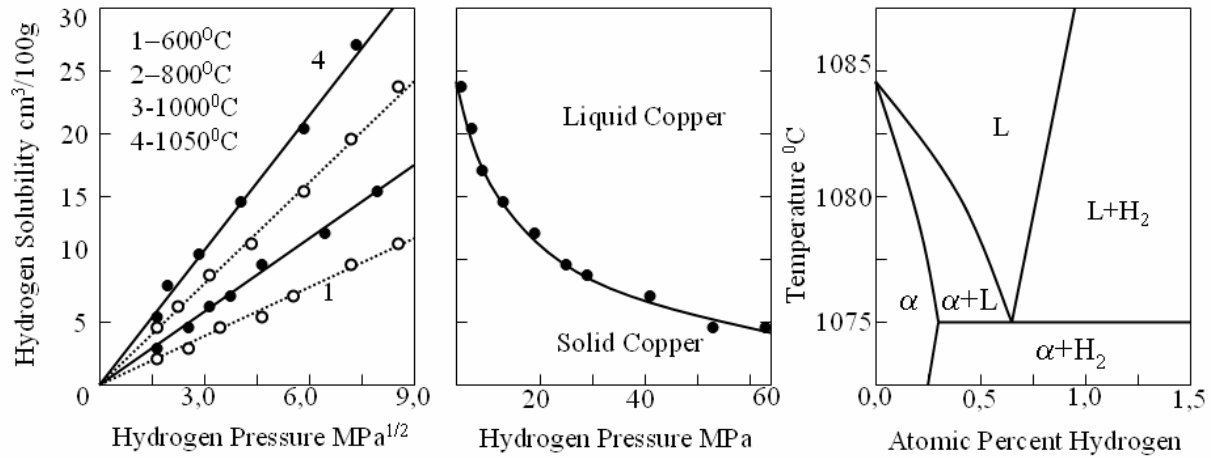


Figure 12. Effects of pressure and temperature on dissolved hydrogen content in copper. 1: 600 °C, 2: 800 °C, 3: 1000 °C, 4: 1050 °C.

Figure 13. Influence of hydrogen pressure on copper melting temperature.

Figure 14. Cu-H phase diagram for pressures up to 50 MPa.

Rising hydrogen pressure in the furnace and accordingly hydrogen content of copper results in monotonous lowering of the melting temperature, Fig. 13. However, the influence of hydrogen is comparatively weak because of its low solubility in and relatively weak interactions with copper.

The experimental data were used to determine a partial phase diagram for the Cu-H system, Fig. 14. Clearly, the system exhibits gas-eutectic equilibrium in the vicinity of the melting point for pure copper.

### The Systems Aluminum-Hydrogen and Magnesium-Hydrogen

Magnesium and aluminum have a wide variety of applications in aerospace, nuclear engineering and chemical processing industry, which invites more data on thermodynamic characteristics of the Mg-H and Al-H systems.

The available data for magnesium are quite insufficient and often contradictory [10-13]. For example, one paper cited exothermic hydrogen occlusion by magnesium while another found it to be endothermic. It is not our intention to make a survey of the literature, for it is presumed that the contradictions in the data mostly result from methodological errors which are especially common in studies into hydrogen behavior in metals.

The solubility of hydrogen in aluminum was studied by many researchers, and their data are in good agreement [14]. For this reason, no attempt was made to investigate hydrogen solubility in aluminum while the most reliable literature data were utilized for determination of a partial phase diagram.

Hydrogen solubility in magnesium was measured at pressures up to 60 MPa using the above techniques. Fig. 15 gives results obtained at a pressure of 0.1 MPa. As the pressure is increased to 60 MPa, the solubility rises also, obeying the Sieverts law. This type of behavior is observed in the Al-H system as well. In this regard, magnesium and aluminum are fairly similar to copper.

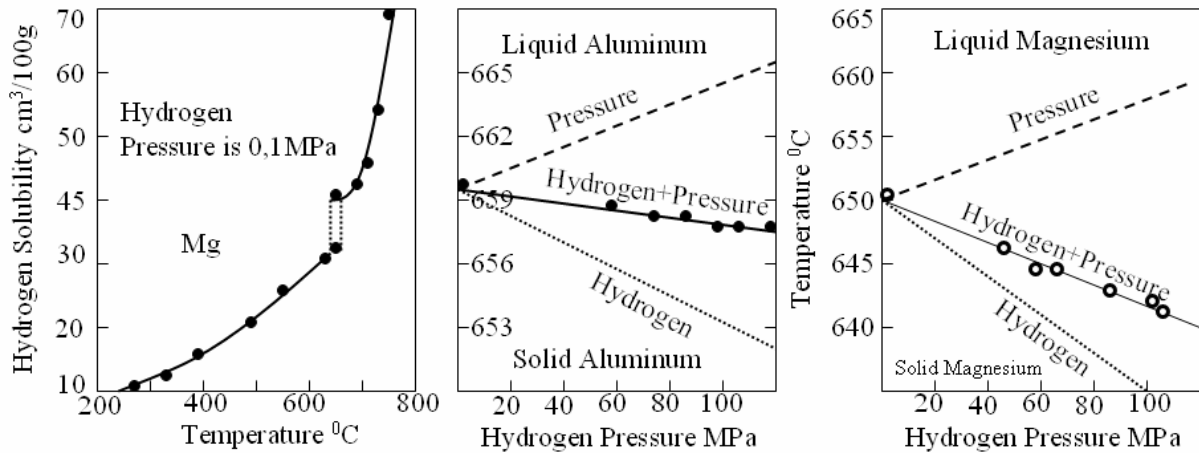


Figure 15. Hydrogen solubility in magnesium at 0.1 MPa pressure.

Figure 16. Melting temperature of aluminum (top) and magnesium (bottom) as a function of hydrogen pressure (dots), uniform compression (dotted lines) and dissolved hydrogen content alone (solid lines).

The experiments on melting in hydrogen gas revealed that hydrogen dramatically reduces melting temperature of magnesium but has negligible effect on aluminum, Fig. 16. Note that with magnesium the influence of hydrogen is appreciable below 15 MPa while above that pressure, the drops in melting temperature are very low.

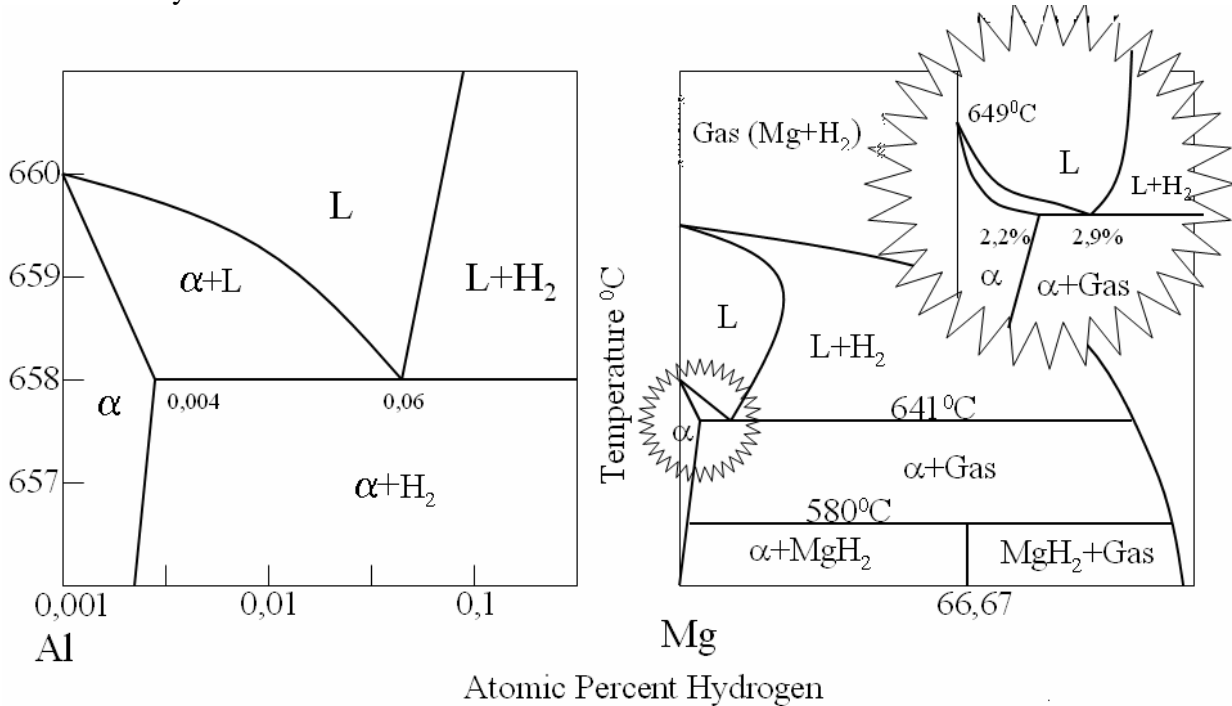


Figure 17. Phase diagrams of the Al-H system for 100 MPa hydrogen pressure (left) and the Mg-H system for 0.1 MPa pressure (right).

This behavior results from simultaneous action of uniform compression that increases the melting temperature and solute hydrogen that lowers it, the two factors being mutually balanced in a high-pressure melting run. The influence of hydrogen per se is felt up to 100 MPa.

With aluminum, a small 2 K drop in melting temperature is observed as the pressure is increased to 90 MPa. So slight an effect is largely due to the very low solubility of hydrogen in aluminum. For this reason, the uniform compression balances out the impact of dissolved hydrogen almost completely.

Based on the experimental data and the available conditions of magnesium hydride occurrence, phase diagrams were constructed for the systems Mg-H and Al-H, Fig. 17. The Mg-H phase diagram involves two invariant equilibria, namely a gas-eutectic and a gas-peritectoid one associated with hydride decomposition in heating. The Al-H diagram, however, displays only a gas-eutectic equilibrium. As regards possibility of aluminum hydride formation, no reliable data are available in the literature.

### The Manganese-Hydrogen System

Manganese is widely used in metallurgy. However, such data are extremely scarce. It is not even conclusively established whether this metal absorbs hydrogen exothermally or endothermally [10, 15-17].

The solubility of hydrogen in manganese was investigated at pressures ranging from 0.1 to 50 MPa and temperatures from 300 to 1450 °C in this study. For these purposes, electrolytic manganese with a purity of 99.95 % was remelted in an induction furnace filled with spectroscopically pure helium gas.

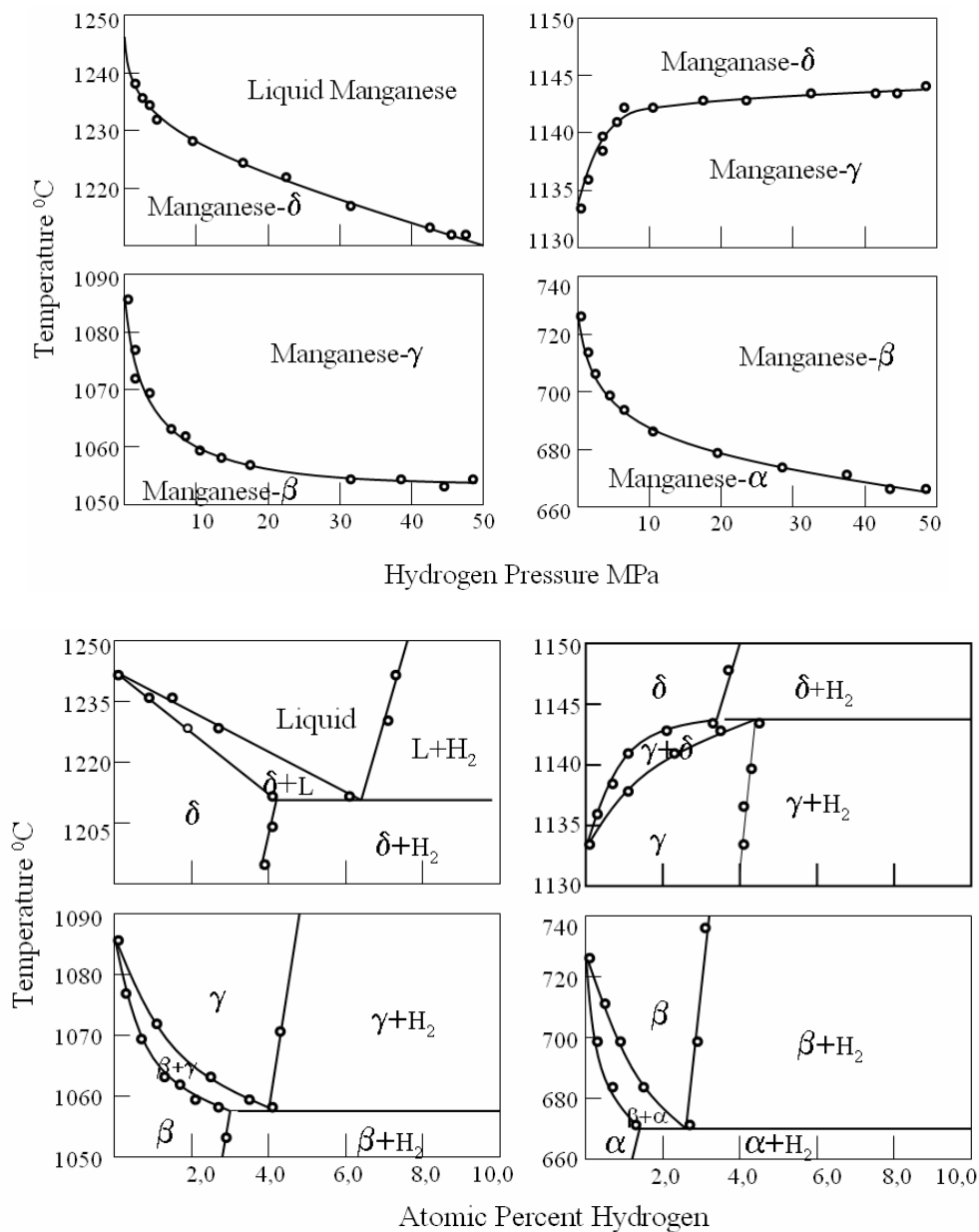


Figure 18. Manganese transformation temperature shifts due to uniform compression (1), hydrogen content alone (pressure (dots) and dissolved hydrogen 2).

Figure 19. Mn-H phase diagram for pressures up to 50 MPa.

The experiments revealed that manganese occludes hydrogen endothermally over the entire temperature range studied. No deviations from Sieverts law were observed — a peculiarity of manganese in comparison to iron, nickel and cobalt. It is probably associated with the close chemical affinity of manganese to hydrogen which enhances the metal's ability to occlude the gas. It is not impossible that negative deviations from Sieverts law will occur at pressures exceeding 50 MPa. So high pressures, however, were beyond the scope of these studies.

A study into the transformation temperatures revealed that hydrogen stabilizes that phase in which it shows the higher solubility, Fig. 18. This refers to the liquid and the solid polymorphs of manganese alike.

The data obtained at pressures up to 50 MPa were used to determine a phase diagram for the Mn-H system, Fig. 19. The diagram exhibits a gas-eutectic, a gas-peritectoid and two gas-eutectoid equilibria. No manganese hydrides were either observed in the experiments or mentioned in the available literature.

### The Systems Molybdenum-Hydrogen and Tungsten-Hydrogen

Very little data on the systems Mo-H and W-H were found in the literature [18, 19]. No information was available about research specifically aimed at determining hydrogen solubility in these metals near their melting temperatures.

We investigated hydrogen absorption by liquid tungsten and molybdenum under nearly equilibrium conditions. The experimentation involved a special apparatus in which direct-arc crucibleless melting in a controlled atmosphere was followed by melt quenching in a water-cooled copper mold.

The unit was so designed that the electrodes could be placed in any desired position with respect to the gravitational field. The arc was struck by contacting the electrodes whose dimensions and positions were selected so that all molten metal remained in the arc zone. A drop detached from the electrode and fell into the mold when its weight exceeded the surface tension forces. At this moment, the arc was extinguished. The melt exposure to arc heating was controlled by manipulation of current and electrode dimensions. The apparatus was sealed, vacuum evacuated down to 0.1 Pa and backfilled with a hydrogen-argon mixture of preset composition. One electrode, normally the cathode, was advanced without compromising the autoclave sealing designed for pressures up to 10 MPa.

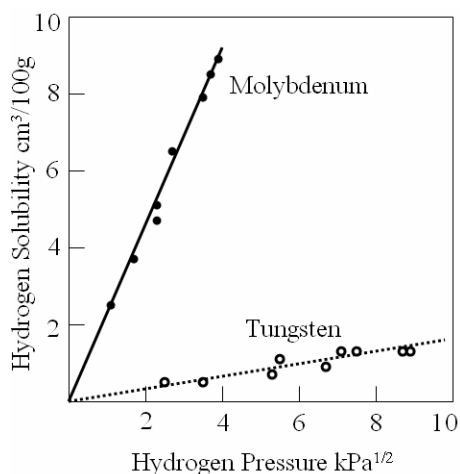


**Figure 20.** Hydrogen solubility in liquid tungsten (1) and liquid molybdenum (2) as a function of hydrogen pressure at melting temperature.

The arc was stabilized with a magnetic field. The arc current and voltage, the gas pressure and the thermocouple readings were recorded with a light-beam oscillograph. A special sight port enabled visual observation. The molybdenum used had a purity of 99.96 % and the tungsten 99.95 %. The samples were saturated with hydrogen in the liquid state, quenched, removed and immediately analyzed for hydrogen by the method described above.

The experiments yielded data on hydrogen solubility in liquid tungsten and liquid molybdenum near their melting temperatures. It was found, among other things, that the dissolved hydrogen content obeys Sieverts law, Fig. 20. At melting temperature and a pressure of 0.1 MPa it equals 20 and 1.8 cm<sup>3</sup> per 100 g for molybdenum and tungsten respectively.

### The Beryllium-Hydrogen System

The literature on hydrogen interactions with beryllium mainly deals with hydride formation. Only a few papers are available that address hydrogen solubility in beryllium [21, 22]. Notably, the experimental data on solubility disagree in regard to both the absolute values and the temperature dependency pattern.

With this in mind, a task was set to investigate hydrogen solubility in solid and liquid beryllium over the broadest possible ranges of temperature and pressure.

Compacted beryllium produced by powder metallurgy and having a void fraction of 0.5 % and a purity of 99.97 % was used in the experimentation. The experimental techniques were same as described in the section on the Fe-H system.

Hydrogen solubility was found to increase with increasing temperature and pressure in alpha and beta beryllium alike, see Fig. 22. In the pressure range studied it obeys Sieverts law. A jump in the solubility is observed that corresponds to the  $\alpha \rightarrow \beta$  transformation, Fig. 23.

The temperature of  $\alpha \rightarrow \beta$  transformation was found to decrease markedly with increasing hydrogen pressure, Fig. 23. Beryllium melting temperature also decreases.

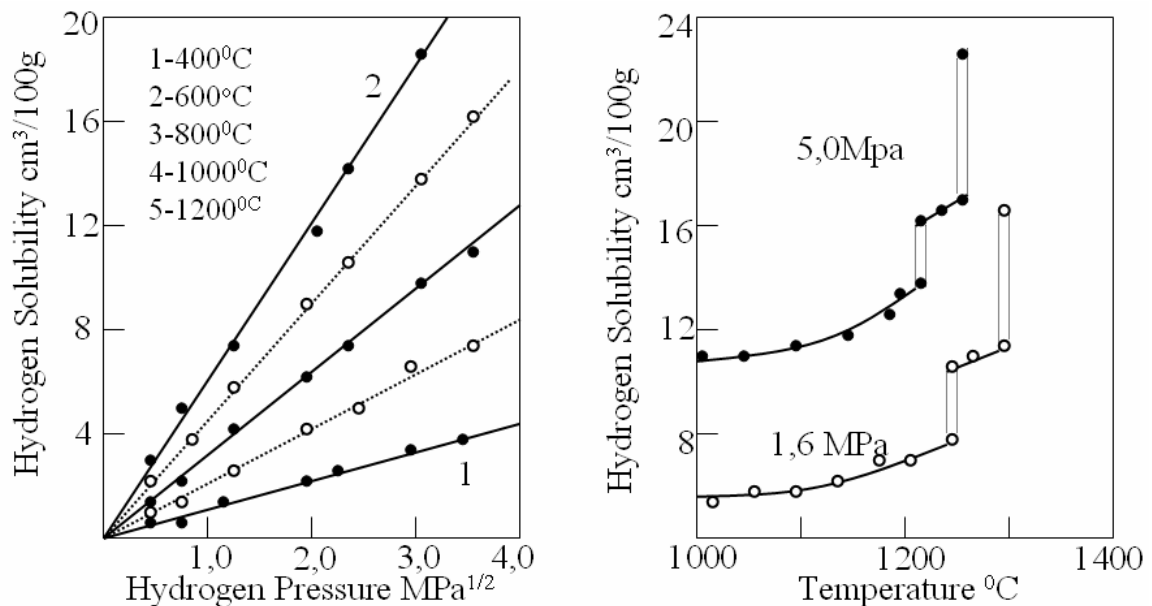


Figure 21. Influence of temperature and hydrogen pressure on hydrogen solubility in beryllium. 1: 1200 °C, 2: 1000°C, 3: 800°C, 4: 600°C, 400°C.

Figure 22. Hydrogen solubility in beryllium as a function of temperature for hydrogen pressures of 1.6 MPa (1) and 5 MPa (2).

Hydrogen solubility in liquid beryllium was only determined for the vicinity of the melting temperature at 12 MPa. The measurements revealed that the solid-liquid transition is accompanied by a jump in hydrogen solubility, Fig. 22. From the data thus obtained, a partial Be-H phase diagram was determined that includes a gas-eutectic and a gas-eutectoid equilibrium, Fig. 24.

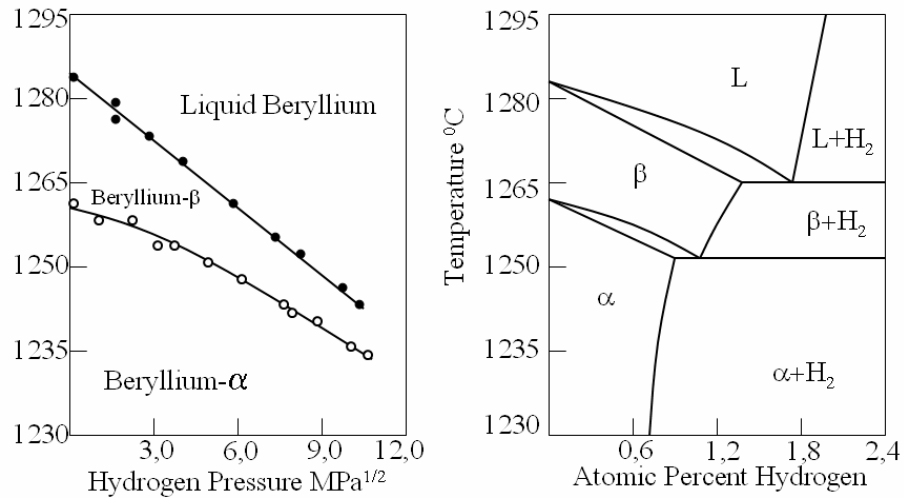


Figure 23. Beryllium transformation temperatures as functions of hydrogen pressure.

Figure 24. Be-H phase diagram for hydrogen pressures up to 5 MPa.

## Conclusions

Summarizing previous findings and the information obtained in our own studies lead to following conclusions:

- The upper portion of phase diagrams for binary metal-hydrogen systems in which the metals absorb hydrogen endothermally at high temperatures displays gas-eutectic equilibrium of the type gas↔liquid solution↔solid solution.
- As an alloying element for iron base alloys, hydrogen is similar to interstitials like carbon, nitrogen and boron in that it stabilizes austenite and narrows stability regions of alpha and delta ferrite.
- In all cases hydrogen lowers metal melting temperatures and also expands stability regions for those polymorphic forms in which it is more soluble.
- The effect of hydrogen on transformation points is primarily dependent on metal chemical nature and normally is increased with increasing solubility.
- Consistent negative deviations from Sieverts law are discovered at high hydrogen pressures, indicating that hydrogen solubility in a crystal lattice is limited and ultimate-solubility phase diagrams must exist for metal-hydrogen systems.

## Acknowledgments

Thanks are due to all colleagues at the “Splav” Laboratory of the State Metallurgical Academy of Ukraine, especially to V.V. Trofimenko, N.P. Serdyuk, V.Yu. Karpov and L.V. Boyko, for their collaboration and participation in challenging experiments. I also thank V.A. Polskii for his unfailing help in preparing my research data for publications and conference presentations.

## References

1. W. Geller, Tak-Hosun, Arch. Eisenhuettenwesen, Bd. 21, S. 423-431, (1950).
2. C.B. Post, R.E. Lake, W.R. Ham, Trans. Amer. Soc. Metals, 27, 530-537, (1939).
3. V.I. Shapovalov, Effects of Hydrogen on Structure and Properties of Fe-C Alloys, Metallurgiya Publishing House, Moscow, 235 p. (1982).
4. V.I. Shapovalov, Izvestiya Vuzov. Chernaya Metallurgiya, No. 12 ( 1976)
5. V.I. Shapovalov, N.P. Serdyuk, Doklady AN Ukr. SSR, No. 2 (1979).
6. L. Luckemeyer-Yasse, H. Shenck, Arch. Eisenhuettenwesen, 1933, Bd. 6, S. 209-220.
7. M.Venkatraman and J.P.Neumann, Journal of Phase Equilibria, Vol.12, No.6, p.672-677 (1991).
8. V.I. Shapovalov, N.P. Serdyuk, Doklady AN Ukr. SSR, 1981, No. 3, p. 88-90.
9. V.I. Shapovalov, N.P. Serdyuk, Izvestiya Vuzov. Tsvetnaya Metallurgiya, , No. 2, 90-93 (1980).
10. A.Sieverts, G. Zapf, H. Moritz, Z. Phys. Chem., Bd. 183, S. 19-30 (1936).
11. Z.D. Popovic, C.R. Piercy, Met. Trans., v. 6A, No. 10, p. 1915-1917 (1975).
12. T. Watanabe, Huang Jenc, B. Komatsu, J. Japan Inst. of Light Metals, , 26, No. 2, p. 76-81 (1976).
13. A.San-Martin and F.D.Manchester, Journal of Phase Equilibria, Vol.13, No.1, p.17-21, (1992).
14. V.I. Shapovalov, N.P. Serdyuk, A.P. Semik, Doklady AN Ukr. SSR, No 6, p. 102-105, (1981).
15. V.I. Shapovalov, N.P. Serdyuk, Izvestiya Vuzov. Chernaya Metallurgiya, , No. 8, p. 70-74 (1982).
16. T. Noda, T. Kainuma, M. Okada, J. Japan Inst. Metals, , v. 48, No. 6, p. 604-610 (1984).
18. S.Ohno, M. Uda, J. Japan Inst. Metals, , v. 48, No. 6, p. 640-646 (1984).
19. V.I. Shapovalov, V.G. Kutsinskii, Doklady AN Ukr. SSR, , No. 11, p. 85-87 (1988).
20. P.M.S. Jones, R. Gibson, Hydrogen in Beryllium, Rep. AWRE-0-2/67., p. 27-33 (1967).
21. V.I. Shapovalov, Yu.M. Dukel'skii, Izvestiya AN SSSR. Metallurgiya, , No. 5, p. 201-203 (1988).

## Keywords

Phase diagrams, solubility, melting temperature, transformation temperature, hydrogen, iron, nickel, cobalt, chromium, magnesium, aluminum, copper, manganese, tungsten, molybdenum, beryllium, high pressures